

Article

## Mo and Mn Co-doping for Isoproturon Degradation Under Visible Light

Yada Yakob<sup>1</sup>, Kanjana Nakhun<sup>1</sup>, Parichat Hirunmas<sup>1</sup>, Paul Egwuonwu Dim<sup>2</sup>, and Mutsee Termtanun<sup>1\*</sup>

<sup>1</sup> Department of Chemical Engineering, Faculty of Engineering and Industrial Technology, Silpakorn University, Nakhon Pathom, 73000, Thailand

<sup>2</sup> Department of Chemical Engineering, School of Infrastructure, Process and Engineering Technology, Federal University of Technology, Minna, Nigeria

\*E-mail: Termtanun\_m@su.ac.th (Corresponding author)

**Abstract.** This research focused on the improvement of the catalytic efficiency of titanium dioxide using transition metals for isoproturon degradation under visible light. Molybdenum and manganese were varied at 0.5% by weight and 1% by weight. Mo/Mn doped TiO<sub>2</sub> was synthesized using sol-gel method and compared with the undoped TiO<sub>2</sub> to find out the most suitable doping metal and doping amount for the degradation of isoproturon, a pesticide generally used in agricultural sites. The characterization techniques for all doped TiO<sub>2</sub> included N<sub>2</sub> physical adsorption/desorption (BET), X-Ray diffraction Spectroscopy (XRD), Ultra Violet -Visible Spectroscopy (UV-VIS), Photoluminescence Spectroscopy (PL), and SEM (Scanning Electron Microscope) –EDX (Energy Dispersive X-ray Diffraction). For each TiO<sub>2</sub> catalyst, the photocatalytic degradation of 10 ppm isoproturon was carried out under visible light and the catalytic efficiency was determined using UV-VIS to measure the residual concentration of isoproturon. According to the results, doping molybdenum and manganese assists in reducing the band gap energy, increasing the surface area of catalysts, and enhancing the photocatalytic activity. In case of manganese, it also minimizes the recombination of photogenerated electrons and holes, which leads to better photocatalytic performance. The optimum isoproturon degradation is appeared with the co-doped Mo and Mn at 1% by weight.

**Keywords:** Photocatalytic degradation, sol-gel technique, isoproturon, molybdenum, manganese.

ENGINEERING JOURNAL Volume 25 Issue 2

Received 7 February 2020

Accepted 25 November 2020

Published 28 February 2021

Online at <https://engj.org/>

DOI:10.4186/ej.2021.25.2.277

*This article is based on the presentation at the International Conference on Engineering and Industrial Technology (ICEIT 2020) in Chonburi, Thailand, 11th-13th September 2020.*

## 1. Introduction

Isoproturon, a herbicide for eliminating biennial grass such as wheat and barley, is highly toxic and easily accumulate in an environment, which is fatal to human and various aqueous creatures even in the minimal amounts. It appears to be acute oral toxicity for rat at approximately 1,800 mg/kg, and acute dermal toxicity for rabbit at greater than 2,000 mg/kg. There is still isoproturon contaminated up to 500 mg per square meter in a residential area, while European union limit drinking water is fixed to 0.1 µg/l [1]. One alternative to remove this compound is using photocatalysis in which isoproturon can be decontaminated by TiO<sub>2</sub>. Generally, titanium dioxide is used as a catalyst in different ways due to its chemical stability, environmentally friendly and inexpensive but an effective working range is only within the ultraviolet light (UV). However, the solar energy is composed of less than 5% UV [2]. Hence, the improvement of TiO<sub>2</sub> catalytic performance has received much attention for organic chemicals treatment under sunlight. There have been several routes to prepare TiO<sub>2</sub>, for example, sol-gel technique, hydrothermal, flame spray pyrolysis, reverse-micelles template, etc. However, the sol-gel method is generally used due to its several advantages. By tailoring the chemical structure of primary precursor and controlling synthesis parameters, sol-gel technique provides nano-sized crystalline materials with high level of chemical purity and photocatalytic activity [3-12]. In this research, TiO<sub>2</sub> catalysts synthesized by sol-gel technique were modified by adding metal to implement the utilization ability of isoproturon degradation under visible light. According to some prior researches, Mo assists in reducing the recombination of photogenerated charge carries, while Mn has the ability to reduce the band gap energy. Therefore, this work was interested in modifying TiO<sub>2</sub> with co-loading of transition metals, molybdenum (Mo) and manganese (Mn), to enhance high photocatalytic activity relating with promoting organic substances removal including isoproturon.

## 2. Materials and Methods

### 2.1. Catalysts Preparation

All catalysts were synthesized by sol-gel method using dissolved titanium (IV) isopropoxide (TTIP) in ethanol. The undoped TiO<sub>2</sub> was prepared by (C<sub>12</sub>H<sub>28</sub>O<sub>4</sub>Ti) dissolving titanium (IV) isopropoxide (TTIP) in ethanol and adding HCl with some distilled water under vigorously stirring at an ambient temperature. The samples were dried in the oven at 80 °C for 24 h and calcined at 500 °C for 3 h with a heating rate of 5 °C/min. [12] While, in case of Mo/Mn doped TiO<sub>2</sub>, TiO<sub>2</sub> was in sol-gel form using titanium tetraisopropoxide (TTIP) dissolved in ethanol as a precursor with 0.5 and 1 wt. % surface deposition of Mo and Mn by adding molybdenum (V) chloride and Manganese (II) chloride tetrahydrate as precursors, respectively.

### 2.2. Catalysts Characterization

In this research, the crystal structures and phase compositions were analyzed using XRD using CuKα radiation between the 2θ range of 20-80 degrees with 2 degree/min. UV-Vis were carried out at the absorption wavelength of 240 nm to measure the remaining concentration of isoproturon. For catalysts powder, UV-Vis were performed to measure the light absorption with visible wavelength from 200 to 800 nm. N<sub>2</sub> adsorption was applied to measure BET surface area with firstly pretreated in helium gas flow of 50 ml/min at 180°C for 4 h. In order to observe the catalysts surface, SEM were carried out at 2500X magnification. The electrons-holes recombination rate of all doped-TiO<sub>2</sub> and undoped were determined by PL spectra measurement with the excitation wavelength at 330 nm.

### 2.3. Photodegradation of Isoproturon under Visible Light

In the photocatalytic degradation, 0.3 g photocatalyst from sol-gel method was added to 200 ml of 10 ppm isoproturon. The reaction mixture was stirred for 4 h using four 45 W lamps as a visible light source (total light intensity equal to 12000 lumen) and samples were collected every 20 minutes until 4 h. The catalysts were then centrifuged to remove from the remaining isoproturon solution. Finally, the residual concentration of isoproturon solution was measured using the UV-Visible Spectroscopy (UV-vis) at the wavelength of 240 nm to further calculate the degradation percentage.

## 3. Results and Discussion

### 3.1. Characterization Results

Table 1 showed the results of BET characterization such as surface area (m<sup>2</sup>/g), mean pore diameter (nm). According to the table, the surface areas of all doped TiO<sub>2</sub> are larger than that of the undoped TiO<sub>2</sub>. The addition of metal leads to an increase of the surface area and a decrease of the mean pore diameter. In case of Mo ions, the specific surface area increased upon the incorporation of Mo since the similarity of Mo<sup>5+</sup> and Mo<sup>6+</sup> ionic radii with Ti<sup>4+</sup> so that they possibly embed into the TiO<sub>2</sub> crystal lattice by isomorphous substitution [13]. For Mn loading, an increase of BET surface area upon the undoped TiO<sub>2</sub> might be caused from more fraction of micropore structure [14]. However, a decreasing of BET surface area with the higher Mn loading is possible due to an incorporation of Mn ions into TiO<sub>2</sub> lattice preserving the anatase phase because of the influence of Mn charge of ionic radius [15]. This can be confirmed with XRD results that a decrease in crystalline size of anatase TiO<sub>2</sub> in Table 2. From Table 1, the pore diameter of the Mo/Mn-TiO<sub>2</sub> catalysts were smaller than those of undoped TiO<sub>2</sub>. However, the mesopores in TiO<sub>2</sub> still appear after doping

both Mo and Mn, creating efficiently photocatalytic reaction [16-18]. Among others, the single doped of Mn 0.5 wt% results in larger surface area at 57.98 m<sup>2</sup>/g with the mean pore diameter at 8.12 nm. The co-doped of 0.5 wt% Mo and Mn provide the largest surface area when compared with other co-doped TiO<sub>2</sub>.

Table 1. BET surface area and pore size of Mo and Mn-doped TiO<sub>2</sub>.

Catalyst samples	BET surface area (m <sup>2</sup> /g)	Mean pore diameter (nm)
Undoped TiO <sub>2</sub>	33.99	11.10
Mo 0.5 wt%	36.99	9.71
Mo 1 wt%	53.16	7.96
Mn 0.5 wt%	57.98	8.12
Mn 1 wt%	54.6	7.53
Mo:Mn=0.5:0.5wt%	34.96	10.20
Mo:Mn=1:1wt%	47.14	9.04
Mo:Mn=0.5:1wt%	39.92	9.71
Mo:Mn=1:0.5wt%	49.13	8.06

From XRD patterns in Fig. 1, the average crystalline size and phase compositions of TiO<sub>2</sub> were calculated according to Debye-Scherrer equation [19] and Scurr-Myers equation [20], respectively. From the results, the average crystalline size of the pure TiO<sub>2</sub> in anatase phase was 17.72 nm, shown in Table 2. After loading Mo and Mn, anatase to rutile ratio increased when compared with undoped which significantly impacted on photocatalytic efficiency, corresponding with the isoproturon degradation results in further section. This confirms with the other research discovered that approximately 60% anatase and 40% rutile exhibits an optimal photocatalytic performance [21]. It is obvious that crystalline size of the anatase decreased with increasing amount of Mn/Mo [22]. This was corresponding with the previous research finding that Mo and Mn significantly reduce the crystalline size of TiO<sub>2</sub> [23, 24].

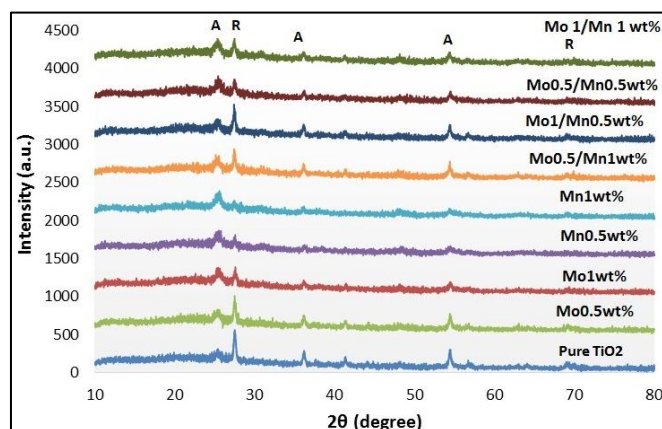


Fig. 1. XRD patterns of different Mo/Mn doped-TiO<sub>2</sub> compared with the undoped TiO<sub>2</sub>.

Table 2. Average crystalline size and phase composition (% anatase and rutile) of Mo/Mn doped-TiO<sub>2</sub> compared with the undoped TiO<sub>2</sub>.

Catalyst samples	Average crystallite size (nm)		Percent (%)	
	Anatase	Rutile	Anatase	Rutile
Undoped TiO <sub>2</sub>	17.72	14.50	24.73	75.27
Mo 0.5 wt%	16.40	17.31	28.94	71.06
Mo 1 wt%	16.46	21.78	43.55	56.45
Mn 0.5 wt%	12.55	10.62	56.94	43.06
Mn 1 wt%	11.30	12.73	58.83	41.17
Mo:Mn=0.5:0.5wt%	16.86	14.32	45.47	54.53
Mo:Mn=1:1wt%	14.29	10.46	60.77	39.23
Mo:Mn=0.5:1wt%	16.71	17.32	64.41	35.59
Mo:Mn=1:0.5wt%	12.96	11.85	59.62	40.38

Table 3. Band gap energy of Mo/Mn doped on TiO<sub>2</sub>.

Catalyst samples	Band gap energy (eV)
Undoped TiO <sub>2</sub>	2.95
Mo 0.5 wt%	2.92
Mo 1 wt%	2.88
Mn 0.5 wt%	2.75
Mn 1 wt%	2.69
Mo: Mn=0.5:0.5 wt%	2.8
Mo:Mn =1:1 wt%	2.64
Mo:Mn=0.5:1wt%	2.57
Mo:Mn= 1:0.5 wt%	2.71

The band gap energy of each TiO<sub>2</sub> was calculated based on Kubelka – Munk relationship [25], shown in Table 3. While comparing among single doped metal, Mn 0.5 wt% doped-TiO<sub>2</sub> has smaller band gap energy (2.75 eV) than Mo 0.5 wt% doped-TiO<sub>2</sub> (2.92 eV) and the undoped TiO<sub>2</sub> (2.95 eV). These results confirmed that type of doping metal influences on the light absorption: doping Mn provides further shift to more visible wavelength when compared with Mo [26]. The loading amount also significantly influences on narrower the band gap energy since the higher the metal loading, the smaller the band gap energy [27]. All co-doped catalysts provide smaller band gap energy than the single metal-doped. Especially, Mo 0.5/Mn 1 wt% doped on TiO<sub>2</sub> allocated the smallest band gap energy (2.57 eV) among all TiO<sub>2</sub> samples.

According to PL characterization in Fig. 2, doping the metals suppresses electrons-holes recombination rate since the defect-rich structural might be induced into TiO<sub>2</sub>, prolonging excitation lifetimes and boosting photocatalytic activity [28, 29]. From Fig. 2, co-doped of Mo and Mn at 1wt% possesses the lowest recombination rate, corresponding to Fig. 4 as it achieved the most isoproturon degradation (37.8%).

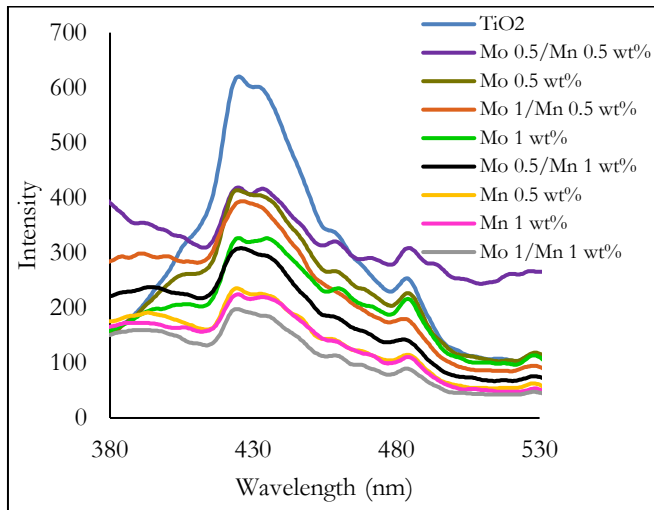


Fig. 2. Photoluminescence spectrum of undoped TiO<sub>2</sub> and doped TiO<sub>2</sub>.

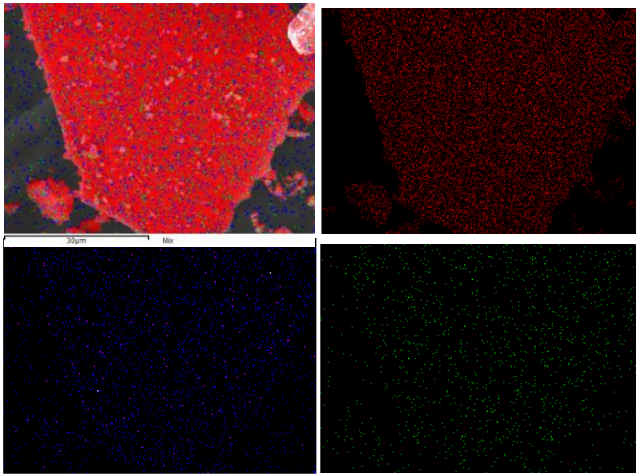


Fig. 3. SEM mapping of 1% co-doping of Mo and Mn on TiO<sub>2</sub> at 2500X magnification, red dots represent Ti, blue dots represent Mo, and green dots represent Mn, respectively.

Moreover, the surface distribution of two doped metals at different doping amounts were also proved using SEM mapping. According to Fig. 3, Mo and Mn were well-dispersed on TiO<sub>2</sub> surface with an insignificant variation [30] (approximately  $\pm 0.07$  from expected doping percentage).

### 3.2. Results of Isoproturon Degradation

The photocatalytic degradation of isoproturon using TiO<sub>2</sub> follows the pseudo first-order linear reaction [31, 32]. The relationship between  $-\ln(C_A/C_{A0})$  versus time is appeared to be linear, therefore the reaction rate constant ( $k$  value), shown in Table 4, can be calculated from Eq. (2).

Degradation rate of isoproturon is assumed to be equal to  $R_A$ ,

$$R_A = -dC_A/dt \quad (1)$$

$$-\ln(C_A/C_{A0}) = kt \quad (2)$$

While  $C_A$  is equal to the remaining concentration of isoproturon measured by UV-Vis, and  $C_{A0}$  is equal to an initial concentration of isoproturon.

Table 4. Initial reaction rate constant of various TiO<sub>2</sub> catalysts in photodegradation of isoproturon under visible light.

Catalyst samples	Reaction rate constant (min <sup>-1</sup> )
Undoped TiO <sub>2</sub>	0.00051
Mo 0.5 wt%	0.00108
Mo 1 wt%	0.00107
Mn 0.5 wt%	0.00143
Mn 1 wt%	0.00124
Mo:Mn= 0.5:0.5 wt%	0.00161
Mo:Mn= 1:1 wt%	0.00167
Mo:Mn= 0.5:1 wt%	0.00129
Mo:Mn= 1:0.5 wt%	0.00180

From Table 4, doping Mo and Mn delivered the faster degradation kinetic as implied by an increase of reaction rate constant with the higher doping amount. Also, Mo and Mn co-doping exhibited the synergistic effect as they both together activate in isoproturon degradation, leading to higher reaction rate constant when compared with single-metal doping. Though Mo 1 wt% - Mn 0.5 wt% has the greatest accelerating the photocatalytic degradation of isoproturon due to its highest initial reaction rate constant, its degradation rate was more decline after 2 hours passed when compared to that of 1 wt% co-doped Mo and Mn on TiO<sub>2</sub>. Therefore, 1 wt% co-doped Mo and Mn on TiO<sub>2</sub> showing the maximum isoproturon degradation, which was equal to 37.8% for 4 hours reaction time, presented in Fig 4.

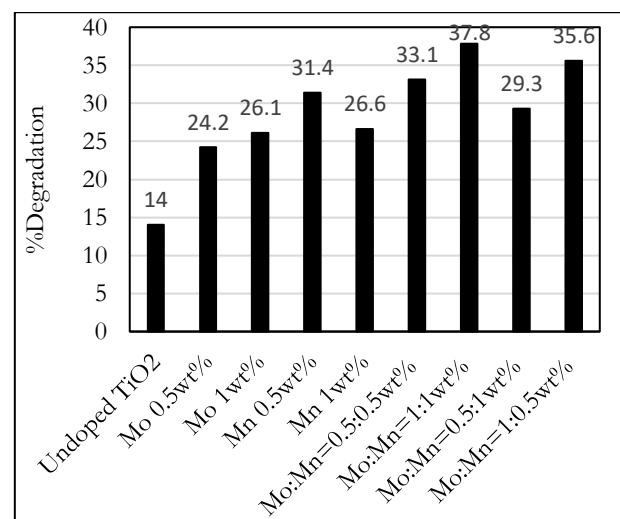


Fig. 4. %Degradation of isoproturon after 4 h under visible light.

Relating to UV-Vis, BET and PL results, doping Mo and Mn on TiO<sub>2</sub> enhances the photocatalytic activity by narrowing the band gap energy, increasing surface area and reducing the recombination rate of electrons and holes. However, there is a threshold limit for decreasing band gap energy as this leads to an increase in electrons-holes recombination rate and destructive the photocatalytic efficiency [33], corresponding with the case of Mo 0.5 wt% and Mn 1wt% on TiO<sub>2</sub> (shown in PL results from Fig. 2 and band gap calculation from Table 3).

#### 4. Conclusions

In this research, Mo and Mn codoped-TiO<sub>2</sub> have successfully been prepared using sol-gel method. The loading metal has significant influence on the photocatalytic activity, surface area, phase composition, crystalline size, band gap energy, and electrons-holes recombination. After Mo and Mn addition on TiO<sub>2</sub>, they both decrease the band gap energy and reduce the electrons-holes recombination when compared with single metal-doped and undoped TiO<sub>2</sub>. In summary, Mo and Mn have synergistic effect on isoprotruron degradation under visible light irradiation. The highest photocatalytic activity in isoprotruron photodegradation (37.8%) belongs to 1 wt% co-doped Mo and Mn on TiO<sub>2</sub>, as its high surface area, high anatase to rutile ratio, small band gap energy, and low electrons-holes recombination. In case of Mo ions, the specific surface area increased upon the incorporation of Mo since the similarity of Mo<sup>5+</sup> and Mo<sup>6+</sup> ionic radii with Ti<sup>4+</sup> so that they possibly embed into TiO<sub>2</sub> crystal lattice by isomorphous substitution [13] which based on the main function of molybdenum in inhibiting the crystal coalescence, presented in another previous research [34]. However, for Mn loading, and an increase of BET surface area upon the undoped TiO<sub>2</sub> might be caused from more fraction of micropore structure [14]. Both Mo and Mn support on the function increasing of TiO<sub>2</sub> surface area, and also reduce the possibility of electrons-holes recombination.

This work is reasonably advantageous for further TiO<sub>2</sub> development as it confirms the synergistic of co-doping of two transition metals on titanium dioxide and also provides an alternative for waste water treatment, especially in case of pesticides removal in agricultural sites.

#### Acknowledgement

This research was financially and instrumentally supported by Department of Chemical Engineering, Faculty of Engineering and Industrial Technology, Silpakorn University, Nakhon Pathom, 73000, Thailand

#### References

- [1] World Health Organization, "Guidelines for drinking-water quality," in *Health Criteria and Other Supporting Information*. 1996.
- [2] Q. R. Deng, X. H. Xia, M. L. Guo, Y. Gao, and G. Shao, "Mn-doped TiO<sub>2</sub> nanopowders with remarkable visible light photocatalytic activity," *Materials Letters*, vol. 65, no. 13, pp. 2051-2054, 2011.
- [3] C. Su, B. -Y. Hong, and C. -M. Tseng, "Sol-gel preparation and photocatalysis of titanium dioxide," *Catalysis Today*, vol. 96, pp. 119-126, 2004.
- [4] V. D. Binas, K. Sambani, T. Maggos, A. anKatsanaki, and G. Kiriakidis, "Synthesis and photocatalytic activity of Mn-doped TiO<sub>2</sub> nanostructured powders under UV and visible light," *Applied Catalysis B: Environmental*, vol. 113, pp. 79-86, 2012.
- [5] M. A. Behnajady, H. Eskandarloo, N. Modirshahla, and M. Shokri, "Investigation of the effect of sol-gel synthesis variables on structural and photocatalytic properties of TiO<sub>2</sub> nanoparticles," *Desalination*, vol. 278, no. 1-3, pp. 10-17, 2011.
- [6] R. Chauhan, A. Kumar, and R. P. Chaudhary, "Structural and photocatalytic studies of Mn doped TiO<sub>2</sub> nanoparticles," *Spectrochim Acta A Mol Biomol Spectrosc*, vol. 98, pp. 256-64, 2012.
- [7] H. Khan and D. Berk, "Characterization and mechanistic study of Mo<sup>+6</sup> and V<sup>+5</sup> codoped TiO<sub>2</sub> as a photocatalyst," *Journal of Photochemistry and Photobiology A: Chemistry*, vol. 294(Supplement C), pp. 96-109, 2014.
- [8] K. Umar, M. M. Haque, M. Muneer, T. Harada, and M. Matsumura, "Mo, Mn and La doped TiO<sub>2</sub>: Synthesis, characterization and photocatalytic activity for the decolourization of three different chromophoric dyes," *Journal of Alloys and Compounds*, vol. 578, pp. 431-438, 2013.
- [9] S. Wang, L. N. Bai, H. M. Sun, Q. Jiang, and J. S. Lian, "Structure and photocatalytic property of Mo-doped TiO<sub>2</sub> nanoparticles," *Powder Technology*, vol. 24, pp. 9-15, 2013.
- [10] Y. Xu, B. Lei, L. Guo, W. Zhou, and Y. Liu, "Preparation, characterization and photocatalytic activity of manganese doped TiO<sub>2</sub> immobilized on silica gel," *Journal of Hazard Materials*, vol. 160, no. 1, pp. 78-82, 2008.
- [11] R. Akbarzadeh and S. Javadpour, "W/Mo-doped TiO<sub>2</sub> for photocatalytic degradation of methylene blue," *International Journal of Engineering Science and Innovative Technology*, vol. 3, no. 4, pp. 621-629, 2014.
- [12] V. Loryuenyong, K. Angamnaysiri, J. Sukcharoenpong, and A. Suwannasri, "Sol-gel derived mesoporous titania nanoparticles: Effects of calcination temperature and alcoholic solvent on the photocatalytic behaviour," *Ceramics International*, vol. 38, no. 3, pp. 2233-2237, 2012.
- [13] M. Cui, S. Pan, Z. Tang, X. Chen, X. Qiao, and Q. Xu, "Physicochemical properties of n-n heterostructured TiO<sub>2</sub>/Mo-TiO<sub>2</sub> composites and their photocatalytic degradation of gaseous toluene," *Chemical Speciation and Bioavailability*, vol. 29, no. 1, pp. 60-69, 2017.
- [14] X. Ma, W. Zhou, and Y. Chen, "Structure and photocatalytic properties of Mn-doped TiO<sub>2</sub> loaded on wood-based activated carbon fiber composites,"

- Materials*, vol. 10, p. 631, 2017, doi: 10.3390/ma10060631.
- [15] P. Junlabhut and P. Nuthongkum, "Structural and optical properties of co-precipitation Mn-doped TiO<sub>2</sub> nanoparticles," *Thai Journal Nanotechnology*, vol. 1, no. 1, pp. 1-7, 2016.
- [16] C. Li, S. Yu, H. Dong, C. Liu, H. Wu, H. Che, and G. Chen, "Z-scheme mesoporous photocatalyst constructed by modification of Sn<sub>3</sub>O<sub>4</sub> nanoclusters on g-C<sub>3</sub>N<sub>4</sub> nanosheets with improved photocatalytic performance and mechanism insight," *Applied Catalysis B: Environmental*, vol. 238, no. 15, pp. 284-293, 2018.
- [17] Y. Castro, N. Arconada, and A. Duran, "Synthesis and photocatalytic characterization of mesoporous TiO<sub>2</sub> films doped with Ca, W and N," *Bulletin of the Spanish Society of Ceramics and Glass*, vol. 54, no. 1, pp. 11-20, 2015.
- [18] B. Niu, X. Wang, K. Wu, X. He, and R. Zhang, "Mesoporous titanium dioxide: synthesis and applications in photocatalysis, energy and biology," *Materials*, vol. 11, no. 10, p. 1910, 2018, doi: 10.3390/ma11101910.
- [19] K. M. Reddy, S. V. Manorama, and A. R. Reddy, "Bandgap studies on anatase titanium dioxide nanoparticles," *Materials Chemistry and Physics*, vol. 78, no. 1, pp. 239-245, 2003.
- [20] D. A. Torres, F. Gordillo-Delgado, and J. Plazas-Saldaña, "Formation of TiO<sub>2</sub> nanostructure by plasma electrolytic oxidation for Cr(VI) reduction," *Journal of Physics: Conf. Series*, vol. 786, p. 012046, 2017.
- [21] R. Su, R. Bechstein, L. So, R. T. Vang, M. Sillassen, B. Esbjornsson, A. Palmqvist, and F. Besenbacher, "How the anatase-to-rutile ratio influences the photoactivity of TiO<sub>2</sub>," *Journal of Physical Chemistry C*, vol. 115, no. 49, pp. 24287-24292, 2011.
- [22] D. A. H. Hanaor and C. C. Sorrell, "Review of the anatase to rutile phase transformation," *Journal of Materials Science*, vol. 46, no. 4, pp. 855-874, 2011.
- [23] M. R. Saidur, A. R. Abdul Aziz, and W. J. Basirum, "Synthesis, characterization and electrochemical study of Mn-doped TiO<sub>2</sub> decorated polypyrrole nanotubes," *IOP Conference Series: Materials Science and Engineering*, vol. 210, p. 012009, 2017, doi: 10.1088/1757-899X/210/1/012009.
- [24] Q. Deng, X. H. Xia, M. Guo, Y. Gao, and G. Shao, "Mn-doped TiO<sub>2</sub> nanopowders with remarkable visible light photoactivity," *Materials Letters*, vol. 65, no. 13, pp. 2051-2054, 2011.
- [25] J. S. Lee, H. K. You, and C. B. Park, "Highly photoactive, low bandgap TiO<sub>2</sub> nanoparticles wrapped by graphene," *Advance Materials Communication*, vol. 24, no. 8, pp. 1084-1088, 2012.
- [26] M. Lesnik, D. Verhovsek, N. Veronovski, M. Gracner, G. Drazic, K. Z. Soderznic, and M. Drogenik, "Hydrothermal synthesis of Mn-doped TiO<sub>2</sub> with a strongly suppressed photocatalytic activity," *Materials and Technology*, vol. 52, no. 4, pp. 411-416, 2018.
- [27] Z. Dargahi, H. Asgharzadeh, and H. Maleki-Ghaleh, "Synthesis of Mo-doped TiO<sub>2</sub>/reduced graphene oxide nanocomposite for photoelectrocatalytic applications," *Ceramics International*, vol. 44, pp. 13015-13023, 2018.
- [28] W. Xie, R. Li, and Q. Yu, "Enhanced photocatalytic activity of Se-doped TiO<sub>2</sub> under visible light irradiation," *Scientific Reports*, vol. 8, no. 1, 2018, doi: 10.1038/s41598-018-27135-4.
- [29] W. Choi, J. Y. Choi, and H. Song, "Regulation of electron-hole recombination kinetics on uniform metal-semiconductor nanostructures for photocatalytic hydrogen evolution," *APL Materials*, vol. 7, p. 100702, 2019, doi: 10.1063/1.5099666.
- [30] R.-G. Ciocarlan, E. M. Seftel, M. Mertens, A. Pui, M. Mazaj, N. N. Tusar, and P. Cool, "Novel magnetic-nanocomposites containing quaternary ferrites systems Co<sub>0.5</sub>Zn<sub>0.25</sub>M<sub>0.25</sub>Fe<sub>2</sub>O<sub>4</sub> (M=Ni, Cu, Mn, Mg) and TiO<sub>2</sub> anatase phase as photocatalysts for wastewater," *Materials Science and Engineering: B*, vol. 230, pp 1-7, 2018.
- [31] A. Verma, N. T. Prakash, and A. P. Toor, "Photocatalytic degradation of herbicide isoproturon in TiO<sub>2</sub> aqueous suspensions: study of reaction intermediates and degradation pathways," *AICHE: Environmental Progress and Sustainable Energy*, vol. 33, no. 2, 2014, DOI: 10.1002/ep.11799.
- [32] S. Thomas, A. Alatrche, M.-N. Pons, and O. Zahraa, "Degradation of herbicide isoproturon by a photocatalytic process," *Comptes Rendus Chimie*, vol. 17, no. 7-8, pp. 824-831, 2014.
- [33] J. Moma and J. Baloyi, "Modified titanium dioxide for photocatalytic applications," in *Photocatalysts-Applications and Attributes*. 2018, doi: 10.5772/intechopen.79374.
- [34] O. Karslioglu, X. Song, H. Kuhlenbeck, and H. -J. Freund, "Mo+TiO<sub>2</sub> (110) mixed oxide layer: structure and reactivity," *Topics in Catalysis*, vol. 56, no. 15-17, pp. 1389-1403, 2013, DOI 10.1007/s11244-013-0142-y.

**Yada Yakob**, photograph and biography not available at the time of publication.

**Kanjana Nagnun**, photograph and biography not available at the time of publication.

**Parichat Hirunmas**, photograph and biography not available at the time of publication.

**Paul Egwuonwu Dim**, photograph and biography not available at the time of publication.

**Mutsee Termtanun**, photograph and biography not available at the time of publication.